51.5 Tb/s Capacity over 17,107 km in C+L Bandwidth Using Single-Mode Fibers and Nonlinearity Compensation

Jin-Xing Cai, *Fellow, IEEE, Fellow, OSA*, Hussam G. Batshon, *Member, IEEE*, Matthew V. Mazurczyk, Oleg V. Sinkin, *Senior Member, IEEE*, Ding Wang, Milen Paskov, *Member, IEEE*, Carl R. Davidson, *Senior Member, IEEE*, William W. Patterson, Alexey Turukhin, Maxim A. Bolshtyansky, and Dmitri G. Foursa, *Senior Member, IEEE*

(Invited Paper)

***Abstract*—We transmit 51.5 Tb/s capacity over 17,107 km with C+L band erbium doped fiber amplifiers (EDFAs) and demonstrate a record single mode fiber capacity-distance product of 881 Pb/s × km. This is achieved by using a performance optimized multidimensional coded modulation format with hybrid probabilistic and geometric constellation shaping. This 4D-PS-7/12-40APSK modulation format is designed to approach the Shannon limit and to maximize the performance of nonlinearity compensation in comparison to conventional and probabilistically shaped two-dimensional formats. The receiver digital signal processing uses multistage nonlinearity compensation that includes fast least-mean-square equalizer and generalized filter in addition to digital back propagation. Adaptive linear filters are aided by coded modulation decisions. We experimentally study the contribution of each algorithm versus transmission distance and show a steady increase in the total nonlinearity compensation benefit up to ∼10,000 km and saturation afterwards. An average total nonlinearity compensation benefit of 1.75 dBQ is achieved after 17,107 km over a 80 nm optical bandwidth at the designed amplifier power. In addition, we show that nonlinearity compensation techniques used in our experiments are not affected by potential correlation among neighboring channels.**

***Index Terms*—Amplitude phase shift keying (APSK), coherent communication, coherent detection, constellation shaping, nonlinearity compensation (NLC), optical fiber communication, wavelength–division multiplexing (WDM).**

I. Introduction

THE first transpacific optical cable connecting the US and Japan was built in 1989 using optical regenerators and operated at 1300 nm with a total capacity of 560 Mb/s (2 fiber pairs × 280 Mb/s) [1]. In less than 30 years, the state-of-the-art transpacific optical cable system, Pacific Light Cable Network (PLCN, connecting HK China and LA US), can carry 144 Tb/s (6 fiber pairs × 24 Tb/s) over ∼13,000 km [2], an increase of more than 250,000 times. PLCN is enabled by the latest technology breakthroughs including digital coherent technology and broadband C+L band amplification. Further increase in single mode fiber (SMF) capacity is very challenging and limited by significant amplified spontaneous emission (ASE) noise and nonlinear noise buildup over transpacific distance [3]. Hence, it is attractive to explore modulation formats with higher receiver sensitivity, better system designs to reduce both linear and nonlinear noise, and advanced DSP schemes to mitigate nonlinear noise induced penalty.

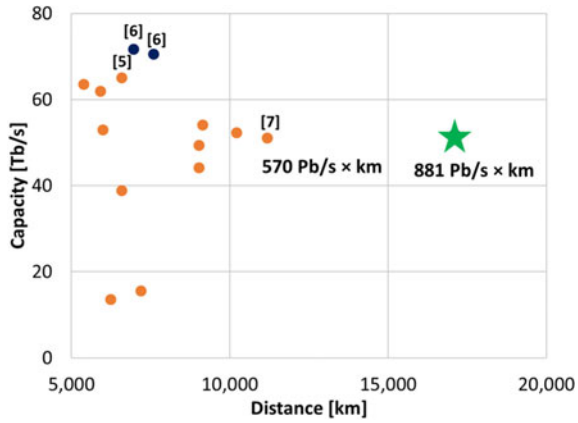

Fig. 1. Laboratory demonstrated single mode fiber capacities over transoceanic distances.

Fig. 1 summarizes record capacity demonstrations in SMF over transoceanic distances since the inception of digital coherent technology, showing that the achievable capacity reduces as transmission distance increases. The record SMF capacity over transoceanic distance of ∼70 Tb/s is demonstrated after 7,000 km [4], while the record capacity-distance product of 881 Pb/s × km is achieved with 51 Tb/s over 17,100 km [5]. Advancements in state of the art digital signal processing (DSP) and nonlinear compensation [6], [7] (and references therein), novel

Manuscript received December 8, 2017; revised January 29, 2018; accepted February 1, 2018. Date of publication February 5, 2018; date of current version March 7, 2018. *(Corresponding author: Jin-Xing Cai.)*

The authors are with the TE Subsea Communications LLC, Eatontown, NJ 07724 USA (e-mail: jcai@subcom.com; hbatshon@subcom.com; mmazurczyk@subcom.com; osinkin@subcom.com; ding.wang@subcom.com; mpaskov@subcom.com; cdavidson@subcom.com; wpatterson@subcom.com; aturukhin@subcom.com; mbolshtyansky@subcom.com; dfoursa@subcom.com).

Color versions of one or more of the figures in this paper are available online at http://ieeexplore.ieee.org.

Digital Object Identifier 10.1109/JLT.2018.2802322

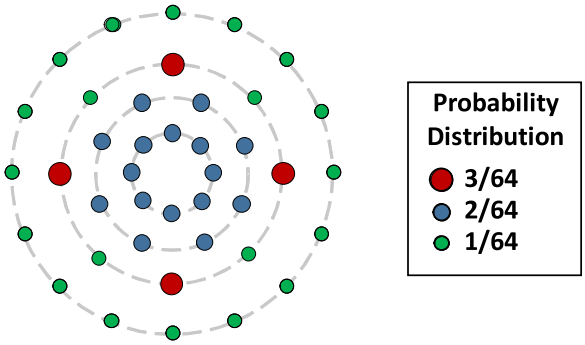

Fig. 2. 2D projection of the 4D-PS-7/12-40APSK constellation diagram.

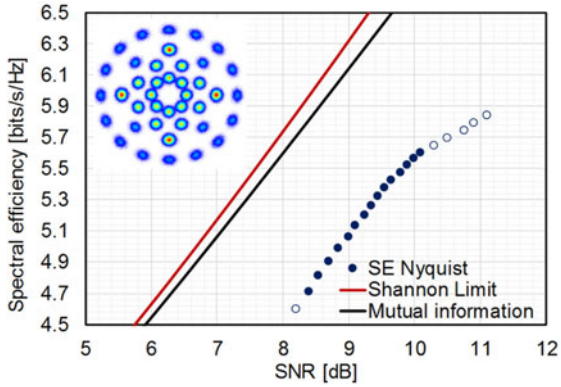

Fig. 3. Shannon limit, 2D mutual information of 4D-PS-7/12-40APSK, and Nyquist SE of 40APSK with implemented 21 adaptive rate FECs (only filled circles are used in the capacity measurements).

modulation formats [8], [9] with spectral efficiency $\gtrsim$8 bits/s/Hz [10], [11], new transmission fibers [12], [13], and the use of broadband amplification [14]–[17] have enabled recent laboratory SMF capacity achievements [4], [5], [14]–[17].

In this paper, we review the latest capacity-distance product record of 881 Pb/s $\times$ km achieved in 51.5 Tb/s transmitting over 17,107 km of SMF using C+L band erbium doped fiber amplifiers (EDFAs) [5]. Section II summarizes the coded modulation scheme, transmitter DSP, receiver DSP, and the nonlinearity compensation (NLC) algorithms used in the work that include digital back propagation (DBP), fast least-mean-square (LMS) equalizer and generalized filter (GF). Section III details the experimental setup and describes the transmitter, the receiver and the transmission testbed. Section IV presents the transmission results. We first present transmission results obtained across the full transmission bandwidth. We then present results of pre-emphasis study showing that the system operates near the nonlinear optimum followed by analysis of nonlinearity compensation benefits of all three schemes above over different transmission distances. In Section V, we address a growing concern related to a possible laboratory transmission measurement inaccuracy resulting from the limited number of uncorrelated modulation paths typically used in experiments [18]. We show that capacity measurements and nonlinearity compensation techniques in this work are not affected by potential correlations between channels.

II. Coded Modulation With Hybrid Shaping, Transmitter and Receiver DSP

A. Coded Modulation With Hybrid Shaping

Constellation shaping, including geometric shaping (GS) and probabilistic shaping (PS), improves the power efficiency of modulation formats and reduces the performance gap with respect to the *linear* Shannon limit. We have proposed and tested two formats, 56APSK [4], [19] and 40APSK [5], where GS with PS are combined in hybrid shaping (HS). In this paper we will discuss the HS 40APSK.

The format uses 5 redundant bits in 2 consecutive symbols (12 bits) for coded modulation. The projection of the constellation diagram in 2D space of the 40APSK is shown in Fig. 2 where the legend shows the probability of occurrence for each constellation point. There are 4 rings in the constellation with equal probability of occurrence (1/4), and the radii are optimized to improve the power efficiency of the modulation format via geometric shaping based on Gaussian distribution [20]. The ratios of the radii from inner to the outer rings are 1, 1.88, 2.71 and 3.95 respectively. This format uses the nonlinear 7/12 code to maximize the minimum Euclidean distance in the 4D-space, resulting in a variable probability distribution of constellation points. The encoding of the 7/12 nonlinear code is similar to that of the 9/12 nonlinear code, and the encoding process can be found in [19]. The two inner rings are composed of 8 equiprobable points each, the third ring is composed of 8 points with two different probability distributions, and the outer ring is composed of 16 equiprobable points. Maximizing the minimum Euclidean distance in 4D-space improves the quality of the feedback signal to the fast LMS equalizer and generalized filter nonlinear compensators. Similarly, the inverse of the 7/12 code is used for 4D decisions and for maximum *a posteriori* (MAP) equalizer in iterative decoding in the receiver.

GS is used to maximize the power efficiency while PS is used to maximize the minimum Euclidean distance in 4D-space to reduce the symbol error ratio (SER). GS is achieved without any redundancy. At the same time, all redundancy is used by PS to introduce a structure in the transmitted signal that improves the Euclidian distance and reduces SER, which in turn improves the quality of the feedback signal to the nonlinear compensators [4], [19].

B. Format Performance

Fig. 3 shows the mutual information (MI) for HS 40APSK (blue line) as a function of signal-to-noise ratio (SNR) in comparison with the Shannon limit. The MI (in two polarizations) is calculated over 2D space (in-phase and quadrature components of the constellation) using Monte Carlo simulation with sufficient statistics. The HS 40APSK is 0.18 dB away from the Shannon limit at 5 bits/s/Hz.

Fig. 3 also shows the Nyquist spectral efficiency of the 4D-PS-7/12-40APSK when combined with adaptive rate forward error correction (FEC) codes using information shortening and parity puncturing [21]. The discrete Nyquist spectral efficiency

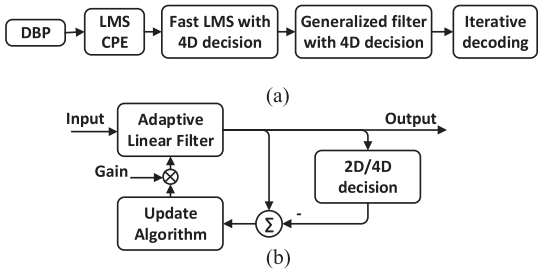

Fig. 4. (a) Receiver DSP chain and (b) Fast LMS with 4D decision.

(SE) points are calculated by estimating the error correction threshold (the SNR required to achieve 10^{-15} at the output of the FEC decoder) for each different FEC overhead; both the FEC overhead and the nonlinear code overhead are accounted for. Similar to [4], [19], the information bits are encoded using a fixed overhead low density parity check (LDPC) code. We use the adaptive-rate decoding [21], [22] to maximize the capacity of channels based on their performance. LDPC overheads from 19.9% to 52% are achieved with variable step size ranging from 1% to 3.5% using information shortening and parity puncturing. Among the 21 designed overheads, 15 (48% to 25%) are used in the capacity experiment. The corresponding Nyquist spectral efficiency ranges from 4.7 to 5.6 bits/s/Hz, and the channel data rate ranges from 154.2 to 182.7 Gb/s. The difference of the required SNR of the adaptive rate FEC implementation from the Shannon limit varies slightly with spectral efficiency and ranges from 2.17 to 2.34 dB with an average of 2.23 dB.

C. Receiver DSP and Nonlinearity Compensation

The receiver DSP (Fig. 4(a)) is designed similarly to [4], [23], and is comprised of both standard optical coherent techniques to compensate for linear transmission effects as well as algorithms which target nonlinear (Kerr) effects. The received samples are first processed with a standard DBP in which the nonlinear compensation factor is experimentally optimized to account for variations in path average power. The traditional DSP chain [24], [25] (and references therein) continues with chromatic dispersion compensation (for the cases without DBP), clock recovery, polarization mode dispersion compensation, carrier frequency offset compensation, carrier phase estimation and *standard* decision directed (DD) LMS.

Nonlinear capacity limit remains the main constraint for spectral efficiencies achievable with advanced modulation formats. DSP techniques that compensate or mitigate the effects of fiber nonlinearities are important tools to increase both capacity and reach. We apply a combination of techniques to compensate for nonlinear transmission effects. Single channel DBP [6], [7] (and references therein) is performed in 2 steps per span followed by fast LMS equalizer [23], [26] and generalized filter [4], [23]. The combination of techniques results in 1.75 dB average Q-factor gain achieved over the entire optical bandwidth.

The *fast* decision directed LMS algorithm [4], [23] is schematically shown in Fig. 4(b). The *fast* LMS leverages the use of a coded modulation (CM) format to significantly lower the symbol error ratio of hard decisions used within the LMS

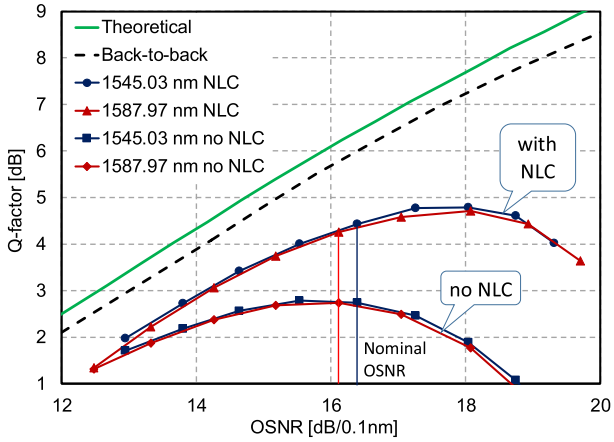

Fig. 5. Theoretical and measured back-to-back performance, and power pre-emphasis curves after 17,107 km for middle C- and L-band channels with and without NLC.

algorithm. CM hard decisions are made by choosing the valid 4D constellation symbol that has the minimum Euclidean distance to the received soft 4D symbol. Because not all pairs of 2D constellation symbols are valid 4D CM symbols, this has the effect of increasing the Euclidean distance and decreasing the symbol error rate. This improves the quality of the LMS error signal, allowing the gain and tracking speed of the LMS filter to be increased and provide compensation of fast varying nonlinear effects.

The generalized filter algorithm [4], [23] estimates correlated nonlinear noise and compensates for it using a time varying linear filter. The assumption is that nonlinear noise is at least partially correlated, and the correlated part can be compensated [27]. The details of estimation of time varying filter coefficients can be found in [4], [23]. In this work, we use an averaging window of approximately 350 and a filter length of 5 taps.

The demodulated symbols at the end of the DSP chain are sent to the iterative decoder [15] where 5 inner LDPC iterations and 10 outer iterations between the MAP decoder and LDPC decoders are performed. Even though the information bits are encoded using a fixed overhead LDPC code, we use the adaptive-rate decoding described in [21], [22] to maximize the capacity of channels based on their performance.

D. Back-to-Back Performance

The noise loaded back-to-back (BtB) measurements of the transmitter and receiver are shown in Fig. 5 with theoretical 40APSK performance at 32.6 GBd. There is ~0.5 dB OSNR implementation penalty at 4.5 dBQ. The insert in Fig. 3 shows the 2D projection of the received constellation at 30 dB OSNR.

III. Experimental Setup

A. Nyquist Channel Transmitter and FEC

Fig. 6 shows the schematic of the laboratory transmitter. We use the same transmitter and receiver arrangement as in [4]. The transmitter is divided into two modulation sections. Four odd and four even external cavity lasers (ECLs) are used as signals

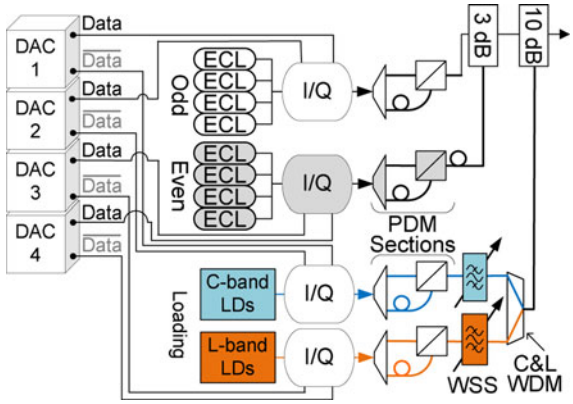

Fig. 6. The schematic of the 295 × 32.6 GBaud Nyquist channel transmitter operating with 40 APSK constellation. DFB: distributed feedback laser, DAC: digital-to-analog converter, DSP: digital signal processing, ECL: external cavity laser, I/Q: in-phase / quadrature-phase, PDM: polarization division multiplexing, PM: polarization maintaining, and WSS: wavelength selective switch.

arranged at 33 GHz spacing. They are modulated at 32.6 Gbaud using I/Q modulators and independent pairs of "I" and "Q" waveforms from 92 GSa/s DACs. Waveforms are generated off-line to produce raised cosine spectra with $\beta = 0.001$. Polarization division multiplexing (PDM) is done with a split and delay technique (∼2600 symbol delay). Odd and even modulators are driven by signals from different DACs with half pattern length shift ensuring the de-correlation between adjacent measurement channels. Channels in the second modulation section are delayed by >3,000 symbols with respect to 8 signal channels. 146 C-band and 149 L-band lasers tuned to the same channel spacing provides loading over the entire 9.74 THz transmission bandwidth. We perform BER measurements on the center 6 of the 8 signal channels that substitute 8 consecutive loading channels. All 295 channels are launched into the circulating loop testbed carrying the same modulation format and symbol rate.

The FEC frames are designed for joint polarization coding. The information bit-stream is a truncated $2^{20}-1$ PRBS pattern that is demultiplexed into 14 data streams. All data streams are independently encoded by identical FEC encoders. The code used is a quasi-cyclic LDPC of length 36,020, girth 8 and column weight 4. The encoded data is first bit-interleaved, then encoded with two identical reversible nonlinear encoders with 7/12 code rate, one for each polarization, and mapped onto 4D symbols (two consecutive 2D symbols). An additional 1.67% symbols are added as pilots to detect and correct cycle slips in the process of carrier phase estimation.

B. Coherent Receiver and Receiver DSP

The coherent receiver is based on a 90° optical hybrid, 200 GS/s digital sampling scopes and offline DSP (Fig. 7). The details of the receiver DSP are discussed in Section II.

C. Circulating Loop Testbed With C+L EDFAs

Fig. 7 shows the schematic of the circulating loop testbed. It consists of twelve 52.8 km fiber spans with 0.150 dB/km loss and $\sim 150\,\mu m^2$ effective area. The chromatic dispersion

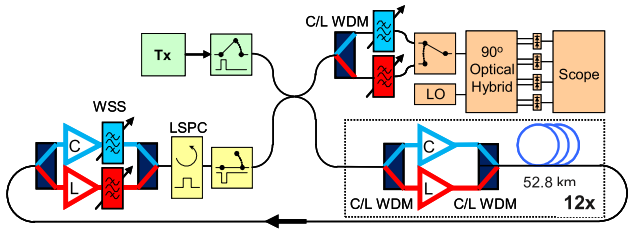

Fig. 7. Coherent receiver and circulating loop testbed using C+L EDFAs with 9.74 THz optical BW. LSPC: loop synchronized polarization controller, WSS: wavelength selective switch.

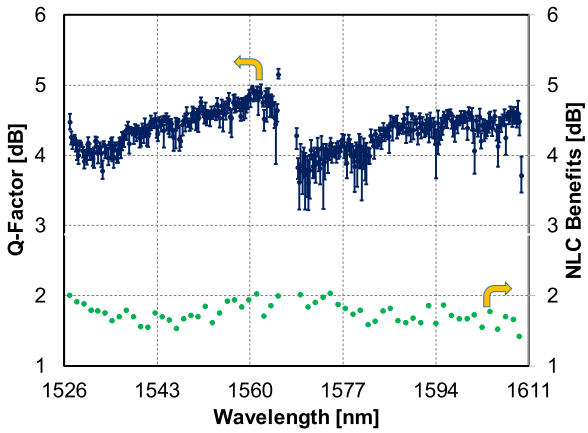

Fig. 8. Q-factor for all channels and NLC benefit for every 5th channel after 17,107 km.

coefficient and dispersion slope at 1550 nm are 20.8 ps/nm/km and 0.062 ps/nm^2/km, respectively; and the total accumulated dispersion after 17,107 km ranges from 331.8 to 417.4 ns/nm. Amplification is provided by C- and L-band EDFAs with the total transmission bandwidth of 9.74 THz. Total C+L band output power is 22.5 dBm launched into the transmission fiber. Residual gain shape of the testbed is compensated by C- and L-band wavelength selective switches (WSS). The system nonlinear performance is maximized by optimizing EDFA output power spectral density and the coded modulation design. Straight-line transmission performance is more accurately represented by using a loop synchronous polarization controller (LSPC). Low speed polarization scanners at the transmitter are used to scan the launched signal polarization.

IV. Transmission Results

A. Capacity Measurements

The average received OSNR for all 295 channels is 16.34 dB/0.1 nm with individual values ranging from 15.2 to 17.3 dB across C- and L-bands after 17,107 km. Q-factors for all channels after 17,107 km are shown in Fig. 8. For each channel of the fully loaded system, we report the polarization averaged BER converted to Q-factor for 10 measurements. Maximum and minimum Q-factor values out of all 10 measurements are shown by error bars. BER for Q-factor calculations is performed after hard decision on the 4D symbols since symbol-by-symbol detection and decoding is not possible with the nonlinear code used in this experiment. At least 15 billion bits have

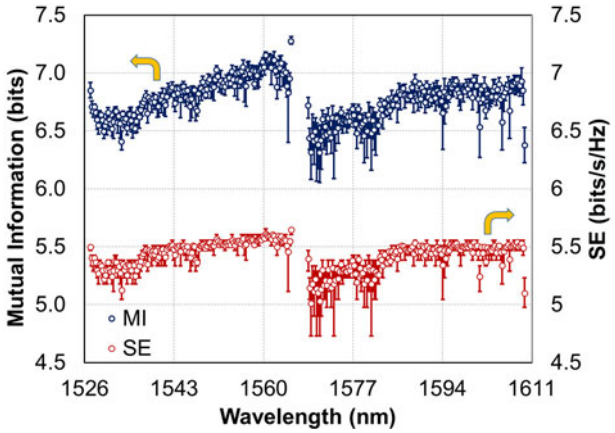

Fig. 9. 2D mutual information and spectral efficiency for all channels after 17,107 km.

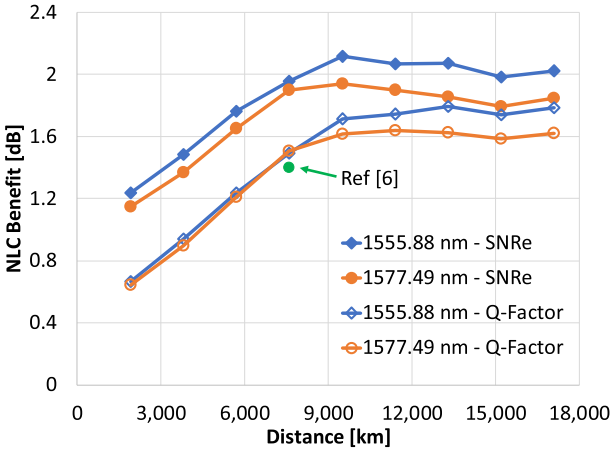

Fig. 10. Nonlinearity compensation benefit in Q-factor and SNRe as a function of transmission distance.

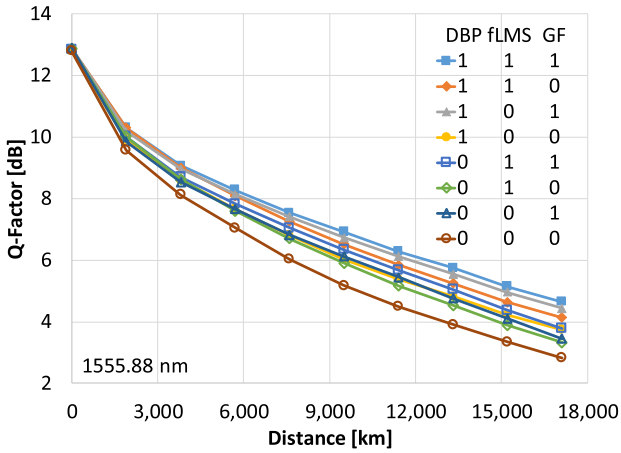

Fig. 11. Performance of different combinations of NLC algorithms after 17,107 km transmission.

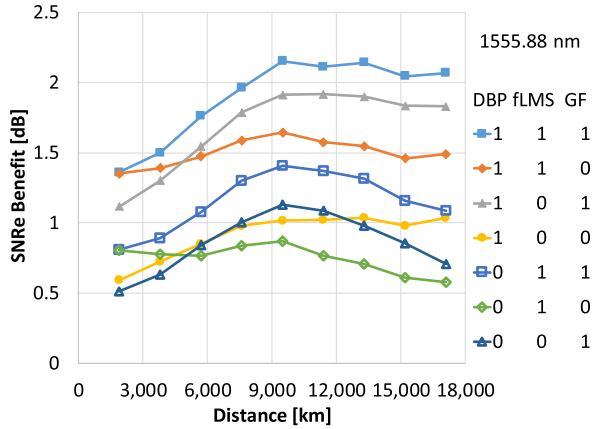

Fig. 12. SNRe benefit using different combination of NLC algorithms relative to without NLC after 17,107 km transmission.

been decoded and all of them are decoded with no errors. We calculate NLC benefit for every 5th channel and plot it in Fig. 8. The average Q-factor benefit using NLC is 1.75 dB resulting in an average effective SNR (SNRe) [28] benefit of 1.96 dB.

The measured 2D MI (in both polarizations) and spectral efficiency for all 295 channels transmitted in C- and L-bands after 17,107 km are shown in Fig. 9. The error bars show the maximum and minimum MI/SE values out of 10 measurements. Figs. 11 and 12 show good correlation between Q-factors and 2D MI in both polarizations.

We achieve a total of 51.51 Tb/s capacity after 17,107 km transmission using 15 out of the 21 code rates shown in Fig. 3. Each channel information bitrate is based on the worst measurement. The channel information rates range from 154.2 to 182.7 Gb/s, and the achieved net spectral efficiency ranges from 4.73 to 5.61 bits/s/Hz with an average of 5.36 bits/s/Hz. The total capacity and the net spectral efficiency reduce to 46.57 Tb/s (287×162.28 Gb/s) and 4.98 bits/s/Hz respectively when no adaptive-rate decoding is used. This demonstrates a gain of 10.6% in system capacity from the use of adaptive rate FEC. The demonstrated capacity corresponds to a record SMF capacity-distance product of 881 Pb/s $\times$ km, representing $>$50% increase over the previous result [17].

B. NLC Benefit

Transmitter pre-emphasis curves after 17,107 km distance are shown in Fig. 5 for middle C-band (1545.03 nm) and middle L-band (1587.97 nm) channels. Pre-emphasis measurements are performed by simultaneously varying the power of 8 contiguous channels of the odd and even rails and measuring the performance of one of the center channels. The acquired data is processed with the decoder set using either only the standard receiver DSP (labeled as 'no NLC') or all three NLC schemes (labeled as 'with NLC'). Both measured channels operate near the peak of the system performance and accumulate similar nonlinear penalties. At the nominal OSNR (with 0 dB pre-emphasis), the average NLC benefit for the two channels is $\sim$1.6 dB. Although Fig. 5 shows that both channels operate $\sim$1.5 dB below optimum OSNR with NLC, we confirmed experimentally that these channels with NLC were operating very close to optimum power by varying all in-line EDFA powers from 21.5 dBm to 23.5 dBm in 0.5 dB steps. The pre-emphasis technique typically shows a peak performance at higher launch powers compared to conditions where the total EDFA power is varied [29].

We measure Q-factors of two channels in the C- and L-bands as a function of transmission distance and calculate the NLC

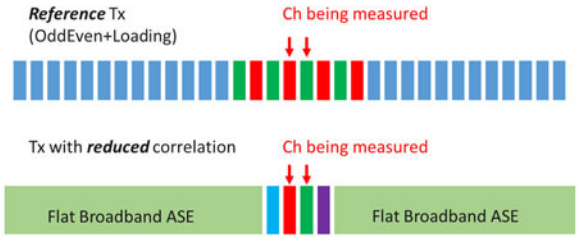

Fig. 13. Two different transmitter channel arrangement schemes used in performance comparisons.

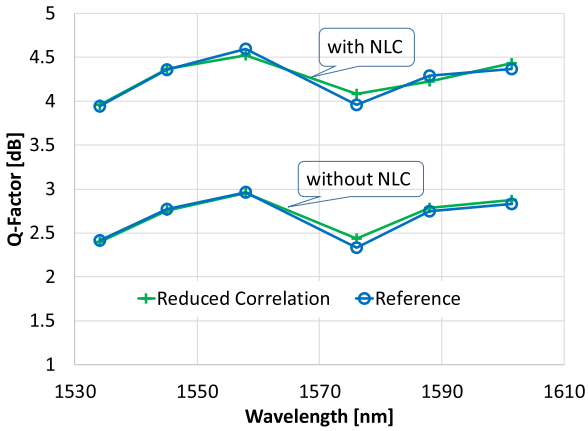

Fig. 14. Performance comparison after 17,107 km for three different transmitter measurement schemes.

benefit (Fig. 10) in both Q-factor and SNRe. Measured Q-factors and the back-to-back curve in Fig. 5 are used for SNRe calculation. SNRe takes ASE noise and noise-like nonlinear distortions from a transmission line into account but excludes limitations from transmitter and receiver hardware implementations [28]. NLC benefit increases with distance up to ∼10,000 km due to increased nonlinearity and limited transmitter and receiver OSNR (28.6 dB/0.1 nm). It is nearly constant for longer transmission distances. The average NLC compensation across the bandwidth achieved in our previous experiment after 7,600 km distance is shown in Fig. 10 as well. It agrees well with the value achieved in the current experiment at a shorter distance.

To get better insights into the NLC contribution of different NLC schemes, we analyze performance of all combinations of the three NLC algorithms versus transmission distance for the same two channels. Performance of the 1555.88 nm channel using different combinations of NLC algorithms is shown in Fig. 11. Corresponding SNRe benefits for all combinations of NLC algorithms are shown in Fig. 12. The same trends are observed for the L-band channel. SNRe benefit from DBP (case '100') increases gradually from 0.6 dB up to ∼1 dB with transmission distance and showing saturation after ∼10,000 km. While showing a higher SNRe benefit at ∼1,900 km (∼0.8 dB), the SNRe benefit of fast LMS (case '010') decreases after 10,000 km. SNRe benefit from GF (case '001') shows a more rapid increase with transmission distance up to 10,000 km, and a gradual decrease afterwards. The maximum SNRe benefit from GF is ∼1.1 dB at ∼10,000 km. Overall, the NLC benefit increases with distance and saturates after ∼10,000 km.

V. Transmitter Induced Channel Correlation

Practical limitations governing laboratory transmitter hardware have typically resulted in a maximum of two independent modulation path arrangement for the signal section. Recent theoretical and experimental studies showed that insufficient decorrelation among WDM channels results in a possible overestimation of nonlinear compensation effect achievable in DSP [18]. Transmission performance without nonlinearity compensation may be affected as well.

We assess performance dependence on possible correlation between the channels and validate the transmission performance using the *Reference* scheme in Fig. 6. This is done by comparing performance of our *Reference* transmitter setup with performance of the transmitter channel arrangement scheme with *Reduced Correlation* (Fig. 13). We decrease channel correlations by using an equalized ASE loading instead of modulated signals in the entire 9.74 THz bandwidth and by substituting 8 Odd/Even channels with two modulation paths with 4 signal channels generated by 4 independent modulation paths with 8 DACs. We ensure that the difference between transmitter OSNRs of the measurement channel is within 0.5 dB for both transmitter arrangements.

We have performed measurements with both transmitter schemes at 6 wavelength allocations across the transmission band. Fig. 14 shows that channel performance (both with and without nonlinearity compensation) are within the measurement accuracy for both transmitter schemes. Moreover, the difference in nonlinearity compensation benefit is within ∼0.1 dB for both schemes. This demonstrates sufficient decorrelation and accuracy of our transmitter setup in 17,107 km experiments. The conclusion drawn from Fig. 14 over 17,107 km transmission distance has been confirmed for different modulation formats like 16 QAM, 40APSK and 56APSK.

VI. Conclusion

We have demonstrated 51.5 Tb/s transmission over a record distance of 17,107 km with 295 × 32.6 Gbaud channels. The demonstrated capacity corresponds to a record SMF capacity-distance product of 881 Pb/s × km representing >50% increase over the previous record. Significant NLC benefit across the transmission bandwidth contributed to this result. The use of multi-stage nonlinear compensation results in an average improvement of 1.75 dB in Q-factor and 1.96 dB in SNRe. These results are achieved by using adaptive-rate decoding applied to 4D-PS-7/12-40APSK based coded modulation with hybrid constellation shaping. We also investigate the separate contributions of our NLC techniques and show a steady increase in the overall nonlinearity compensation benefit up to ∼10,000 km and saturation afterwards. We confirm sufficient decorrelation between the transmitted channels in the experimental setup. It ensures that neither capacity measurements nor NLC techniques in this experiment is affected by correlations among WDM channels.

REFERENCES

[1] N. S. Bergano, *Optical Fiber Telecommunications IIIA*, I. Kaminow and T. Koch, Eds. San Francisco, CA, USA: Academic, 1997, ch. 10.

[2] 2017. [Online]. Available: https://www.submarinenetworks.com/systems/trans-pacific/plcs

[3] P. Poggiolini, "The GN model of non-linear propagation in uncompensated coherent optical systems," *J. Lightw. Technol.*, vol. 30, no. 24, pp. 3857–3879, Dec. 2012.

[4] J.-X. Cai, H. G. Batshon, M. V. Mazurczyk, O. V. Sinkin, D. Wang, M. Paskov, W. Patterson, C. R. Davidson, P. Corbett, G. Wolter, T. Hammon, M. Bolshtyansky, D. Foursa and A. Pilipetskii, "70.46 Tb/s over 7,600 km and 71.65 Tb/s over 6,970 km transmission in C+L band using coded modulation with hybrid constellation shaping and nonlinearity compensation," *J. Lightw. Technol.*, vol. 36, no. 2, pp. 361–371, Jan. 2018.

[5] J.-X. Cai, H. G. Batshon, M. V. Mazurczyk, O. V. Sinkin, D. Wang, M. Paskov, C. R. Davidson, W. W. Patterson, M. A. Bolshtyansky, and D. G. Foursa, "51.5 Tb/s capacity over 17,107 km in C+L bandwidth using single mode fibers and nonlinearity compensation," in *Proc. Eur. Conf. Opt. Commun.*, Gothenburg, Sweden, 2017, Paper Th.PDP.A.2.

[6] J. C. Cartledge, F. P. Guiomar, F. R. Kschischang, G. Liga, and M. P. Yankov, "Digital signal processing for fiber nonlinearities," *Opt. Express*, vol. 25, pp. 1916–1936, 2017, and references therein.

[7] T. Hoshida, "Mitigation of nonlinear propagation impairments by digital signal processing," in *Proc. 42nd Eur. Conf. Opt. Commun.*, Dusseldorf, Germany, 2016, Paper Th1.A.1, and references therein.

[8] F. Buchali, F. Steiner, G. Böcherer, L. Schmalen, P. Schulte, and W. Idler, "Rate adaptation and reach increase by probabilistically shaped 64-QAM: An experimental demonstration," *J. Lightw. Technol.*, vol. 34, no. 7, pp. 1599–1609, Apr. 2016.

[9] M. Karlsson and E. Agrell, "Multidimensional modulation and coding," in *Proc. Opt. Fiber Commun. Conf.*, Anaheim, CA, USA, 2016, Paper M3A.1.

[10] S. Zhang, F. Yaman, Y. Huang, J. D. Downie, D. Zou, W. Wood, A. R. Zakharian, R. Khrapko, S. Mishra, V. Nazarov, J. E. Hurley, I. Djordjevic, E. Mateo, and Y. Inada, "Capacity-approaching transmission over 6375 km at spectral efficiency of 8.3 bit/s/Hz," in *Proc. Opt. Fiber Commun. Conf.*, Anaheim, CA, USA, 2016, Paper Th5C.2.

[11] S. Chandrasekhar, B. Li, J. Cho, X. Chen, E. Burrows, G. Raybon, P. Winzer, "High-spectral-efficiency transmission of PDM 256-QAM with parallel probabilistic shaping at record rate-reach trade-offs," in *Proc. Eur. Conf. Opt. Commun.*, Dusseldorf, Germany, 2016, Paper Th.3.C.1.

[12] Y. Yamamoto, Y. Kawaguchi, and M. Hirano, "Low-loss and low-nonlinearity pure-silica-core fiber for C- and L-band broadband transmission," *J. Lightw. Technol.*, vol. 34, no. 2, pp. 321–326, Jan. 2016.

[13] D. W. Peckham, "Optimization of large area, low loss fiber designs for C+L band transmission," in *Proc. Opt. Fiber Commun. Conf.*, Anaheim, CA, USA, 2016, Paper Tu3G.1.

[14] D. G. Foursa, H. G. Batshon, H. Zhang, M. Mazurczyk, J.-X. Cai, O. Sinkin, A. Pilipetskii, G. Mohs and Neal S. Bergano, "44.1 Tb/s transmission over 9,100 km using coded modulation based on 16QAM signals at 4.9 bits/s/Hz spectral efficiency," in *Proc. Eur. Conf. Opt. Commun.*, London, U.K., 2013, Paper Th.3.E.1.

[15] J.-X. Cai, Y. Sun, H. Zhang, H. G. Batshon, M. V. Mazurczyk, O. V. Sinkin, D. G. Foursa, and A. Pilipetskii, "49.3 Tb/s transmission over 9100 km using C+L EDFA and 54 Tb/s transmission Over 9150 km using hybrid-Raman EDFA," *J. Lightw. Technol.*, vol. 33, no. 13, pp. 2724–2734, Jul. 2015.

[16] A. Ghazisaeidi, I. Fernandez de Jauregui Ruiz, R. Rios-Muller, L. Schmalen, P. Tran, P. Brindel, A. C. Meseguer, Q. Hu, F. Buchali, G. Charlet, and J. Renaudier, "Advanced C+L-Band transoceanic transmission systems based on probabilistically shaped PDM-64QAM," *J. Lightw. Technol.*, vol. 35, no. 7, pp. 1291–1299, Apr. 2017.

[17] S. Zhang, F. Yaman, Y.-K. Huang, J. D. Downie, X. Sun, A. Zakharian, R. Khrapko, W. A. Wood, I. B. Djordjevic, E. Mateo, and Y. Inada, "50.962 Tb/s over 11185 km Bi-Directional C+L transmission using optimized 32QAM," in *Proc. Conf. Lasers Elect.-Opt.*, 2017, Paper JTh5A.9.

[18] R. Dar, S. Chandrasekhar, A. H. Gnauck, B. Li, J. Cho, E. C. Burrows, P. J. Winzer, "Impact of WDM channel correlations on nonlinear transmission," in *Proc. Eur. Conf. Opt. Commun.*, Dusseldorf, Germany, 2016, Paper W.1.D.2.

[19] H. G. Batshon, M. V. Mazurczyk, J.-X. Cai, O. V. Sinkin, M. Paskov, C. R. Davidson, D. Wang, M. Bolshtyansky and D. Foursa, "Coded modulation based on 56APSK with hybrid shaping for high spectral efficiency transmission," in *Proc. Eur. Conf. Opt. Commun.*, Gothenburg, Sweden, 2017, Paper Tu.1.D.2.

[20] Z. Yang, Q. Xie, K. Peng, and Z. Wang, "A novel BICM-ID system approaching Shannon-limit at high spectrum efficiency," *IEICE Trans. Commun.*, vol. E94-B, no. 3, pp. 793–795, 2011.

[21] T. Tian and C. R. Jones, "Construction of rate-compatible LDPC codes utilizing information shortening and parity puncturing," *EURASIP J. Wireless Commun. Netw.*, vol. 5, pp. 789–795, Oct. 2005.

[22] M. Beermann and P. Vary, "Joint optimization of multi-rate LDPC code ensembles for the AWGN channel based on shortening and puncturing," in *Proc. IEEE Wireless Commun. Netw. Conf.*, 2014, pp. 200–205.

[23] M. V. Mazurczyk, J. -X. Cai, H. G. Batshon, M. Paskov, O. V. Sinkin, D. Wang, W. Patterson, C. R. Davidson, P. Corbett, G. Wolter, T. Hammon, M. A. Bolshtyansky, D. G. Foursa, "Performance of nonlinear compensation techniques in a 71.64 Tb/s capacity demonstration over 6,970 km," in *Proc. Eur. Conf. Opt. Commun.*, Gothenburg, Sweden, 2017, Paper Th.2.E.1.

[24] K. Kikuchi, *High Spectral Density Optical Communication Technologies*, M. Nakazawa, K. Kikuchi, and T. Miyazaki, Eds. New York, NY, USA: Springer, 2010, ch. 2, pp. 11–49.

[25] J. X. Cai, K. Golovchenko, and G. Mohs, *Optical Fiber Telecommunications VIB*, I. Kaminow, T. Li, and A. E. Willner, Eds. San Francisco, CA, USA: Academic, 2013, Chapter 25, and references therein.

[26] H. Zhang, C. Davidson, H. Batshon, M. Mazurczyk, M. A. Bolshtyansky, D. Foursa, and A. Pilipetskii, "DP-16QAM based coded modulation transmission in C+L band system at transoceanic distance," in *Proc. Opt. Fiber Commun. Conf.*, Anaheim, CA, USA, 2016, Paper W1I.2.

[27] R. Dar, M. Feder, A. Mecozzi, and M. Shtaif, "Inter-channel nonlinear interference noise in WDM systems: Modeling and mitigation," *J. Lightw. Technol.*, vol. 33, no. 5, pp. 1044–1053, Mar. 2015.

[28] O. Sinkin, C. R. Davidson, H. Wang, L. Richardson, J.-X. Cai, D. Kovsh, D. Foursa, B. Bakhshi, G. Mohs, A. Pilipetskii, "Effective signal to noise ratio performance metric for dispersion-uncompensated links," in *Proc. Eur. Conf. Opt. Commun.*, Valencia, Spain, 2015, Paper P5.3.

[29] O. Sinkin, J. Cai, D. Foursa, G. Mohs, and A. Pilipetskii, "Impact of broadband four-wave mixing on system characterization," in *Proc. Opt. Fiber Commun. Conf. Expo.*, Anaheim, CA, USA, 2013, Paper OTh3G.3.

Authors' biographies not available at the time of publication.